Protist

ORIGINAL PAPER

Asymmetric Cell Division as a Route to Reduction in Cell Length and Change in Cell Morphology in Trypanosomes

Reuben Sharma[a,1], Lori Peacock[b], Eva Gluenz[c], Keith Gull[c], Wendy Gibson[b], and Mark Carrington[a,1]

[a]Department of Biochemistry, University of Cambridge, 80 Tennis Court Road, Cambridge CB2 1GA, UK
[b]School of Biological Sciences, University of Bristol, Bristol BS8 1UG, UK
[c]Sir William Dunn School of Pathology, University of Oxford, South Parks Road, Oxford OX1 3RE, UK

Abstract

African trypanosomes go through at least five developmental stages during their life cycle. The different cellular forms are classified using morphology, including the order of the nucleus, flagellum and kinetoplast along the anterior—posterior axis of the cell, the predominant cell surface molecules and the location within the host. Here, an asymmetrical cell division cycle that is an integral part of the *Trypanosoma brucei* life cycle has been characterised in further detail through the use of cell cycle stage specific markers. The cell cycle leading to the asymmetric division includes an exquisitely synchronised mitosis and exchange in relative location of organelles along the anterior—posterior axis of the cell. These events are coupled to a change in cell surface architecture. During the asymmetric division, the behaviour of the new flagellum is consistent with a role in determining the location of the plane of cell division, a function previously characterised in procyclic cells. Thus, the asymmetric cell division cycle provides a mechanism for a change in cell morphology and also an explanation for how a reduction in cell length can occur in a cell shaped by a stable microtubule array. © 2007 Elsevier GmbH. All rights reserved.

Key words: *Trypanosoma brucei*; asymmetric cell division; differentiation; epimastigote.

Introduction

The cellular form of kinetoplastid protists, such as *Trypanosoma brucei*, is defined by the relative position of three structures: the nucleus, the single flagellum and the kinetoplast which contains the concatenated mitochondrial DNA. Variation of the relative position of these three structures along an anterior posterior axis is used to classify the cell morphological types (Hoare and Wallace 1966). In the trypomastigote form, the kinetoplast lies between the posterior pole and the nucleus whereas in the epimastigote it is positioned between the nucleus and anterior pole (Vickerman et al. 1988). The site of emergence of the flagellum from the cell body is close to the kinetoplast and consequently trypomastigotes have a longer

---

2   R. Sharma et al.

flagellum than epimastigotes as the flagellum overhangs the anterior pole of the cell (Vickerman et al. 1988).

The shape of trypanosome cells is formed by a corset of closely packed subpellicular microtubules (Angelopoulos 1970) that are linked to each other and to the plasma membrane (Hemphill et al. 1991). The only hole in the array of subpellicular microtubules occurs at the point at which the flagellum emerges from the cell body (Hemphill et al. 1991). Individual microtubules within the subpellicular array are stable with little turnover and the cytoskeleton is remarkably constant throughout the cell division cycle (Sherwin and Gull 1989a, 1989b). The differentiation from one cellular form to another occurs without breakdown of the subpellicular microtubule array. This raises the question of whether the new cell morphology can arise by remodelling of an existing single cell or is achieved as part of a division process. The cytoskeleton also has to accommodate growth during proliferative cell cycles when there is an increase in both circumference and length (Robinson et al. 1995). The appearance of new microtubules between old microtubules allows the spacing between the subpellicular microtubules to remain relatively constant as the cell circumference increases (Robinson et al. 1995; Sherwin and Gull 1989b). The increase in cell length is dependent on the extension of microtubules and this occurs mainly at the posterior end of the cell (Robinson et al. 1995).

On infecting a tsetse fly, the mammalian bloodstream trypomastigotes undergo a well characterised differentiation that results in a proliferative population of procyclic trypomastigotes in the insect midgut (Szoor et al. 2006 reviewed in Matthews 2005). Bloodstream form trypanosomes express a variant surface glycoprotein as the dominant cell surface molecule but, during differentiation, the VSG is lost and procyclic cells express procyclins (Roditi et al. 1987, 1989). In addition, procyclics have increased cell dimensions (Vickerman 1985), a different pattern of organelle movement during mitosis (Robinson et al. 1995; Tyler et al. 2001) and use different metabolic pathways for ATP generation (reviewed in Van Hellemond et al. 2005) but retain the trypomastigote morphology. This differentiation occurs over a period of 10—14 h during a G1 cell cycle arrest (Ziegelbauer et al. 1990) and the remodelling of the cell is essentially complete within one cell cycle (Matthews et al. 1995).

As the infection of the tsetse fly progresses within the midgut, trypanosomes move across the peritrophic membrane into the ectoperitrophic space and then migrate to the salivary glands via the foregut, mouthparts and salivary ducts (Lewis and Langridge 1947; Van den Abbeele et al. 1999; Vickerman et al. 1988) (reviewed in Aksoy et al. 2003). During this migration the trypanosomes differentiate from the trypomastigote to the epimastigote morphology during an asymmetric cell division (Lewis and Langridge, 1947; Van den Abbeele et al. 1999). In the salivary glands the epimastigotes attach to the epithelium through an elaboration of the flagellar membrane (Tetley and Vickerman 1985). In addition to the repositioning of the kinetoplast relative to the nucleus, the salivary gland epimastigotes are substantially smaller than procyclic trypomastigotes (Van den Abbeele et al. 1999). The potential to infect a mammal is dependent on a further differentiation of the salivary gland epimastigote to a non-proliferative metacyclic trypomastigote form that is able to establish an infection in a mammal when the fly takes a blood meal (Tetley and Vickerman 1985; Tetley et al. 1987).

Here, the differentiation from midgut trypomastigote to salivary gland epimastigote is re-visited using a variety of molecular probes to enable a more detailed description of the highly asymmetric cell division cycle that starts with a trypomastigote and produces one long and one short epimastigote daughter cell. Analyses of the expression of the sister chromatid cohesin component SCC1, as a marker for S- and G2 phases of the cell cycle, and of procyclin, as a marker for the procyclic form-specific cell surface, were combined with morphometric and electron microscopical approaches. The results show that prior to mitosis during the asymmetric cell division cycle, the cell is in G2 and has a single kinetoplast, a state not normally found in procyclic or bloodstream trypomastigotes. The subsequent division of the kinetoplast is co-incident with nuclear anaphase. The rearrangement of the relative positions of the kinetoplast and nucleus that marks the differentiation of trypomastigotes to epimastigotes is primarily a result of a reduction in the distance between the nucleus and the posterior of the cell, the distance between the posterior and kinetoplast is more or less constant. The division of the kinetoplast is driven by separation of the basal bodies (Ogbadoyi et al. 2003; Robinson and Gull 1991) and the late separation of the basal bodies during the asymmetric cell division correlates with a short new flagellum.

Results

Validation of the Use of anti-SCC1 as a Marker for S and G2 Phases of the Cell Cycle

Eukaryotic chromosomes are replicated during S-phase and the two sister chromatids are separated during mitosis. Between these two events the sister chromatids are held together by cohesin, a protein complex minimally containing four subunits: SMC1, SMC3, SCC3 and SCC1 (reviewed in Nasmyth 2005). In yeast, cohesin is synthesised and assembled onto the replicating chromosomes during S-phase (Lengronne et al. 2006) and the separation of sister chromatids during anaphase is dependent on the proteolysis of SCC1 (Uhlmann et al. 1999). Thus, cells contain SCC1 from the beginning of S-phase until anaphase. Homologues of the four components of cohesin were identified in the *Trypanosoma brucei* genome sequence and a functional analysis of the trypanosome SCC1 demonstrated that it is the orthologue of yeast SCC1 (Gluenz, Sharma, Gull

and Carrington, unpublished results); as part of this work an antiserum that recognised SCC1 was produced (Fig. S1). Immunofluorescence using these antibodies was used to place SCC1 expression within the trypanosome cell division cycle, the stage of individual cells was determined by the nuclear and mitochondrial DNA (kinetoplast) morphology and by detection of bromo-2′-deoxyuridine (BrdU) incorporation into DNA to mark cells in S-phase (Fig. 1). Cells in G1 are characterised by a single nucleus and single kinetoplast (1K1N) and an absence of BrdU incorporation. The majority of these cells were SCC1 negative (Fig. 1a), a small number expressed a small crescent of SCC1 (Fig. 1b) and presumably represented cells about to enter S-phase. Cells in S-phase have one kinetoplast (1K1N) which after replication of the kinetoplast DNA assumes a dumbbell shape. The two foci of BrdU label correspond to the antipodal sites where the replicated minicircles are present. These cells were SCC1 positive and the strength of the SCC1 signal was proportional to the amount of BrdU incorporation (compare Fig. 1c and d).
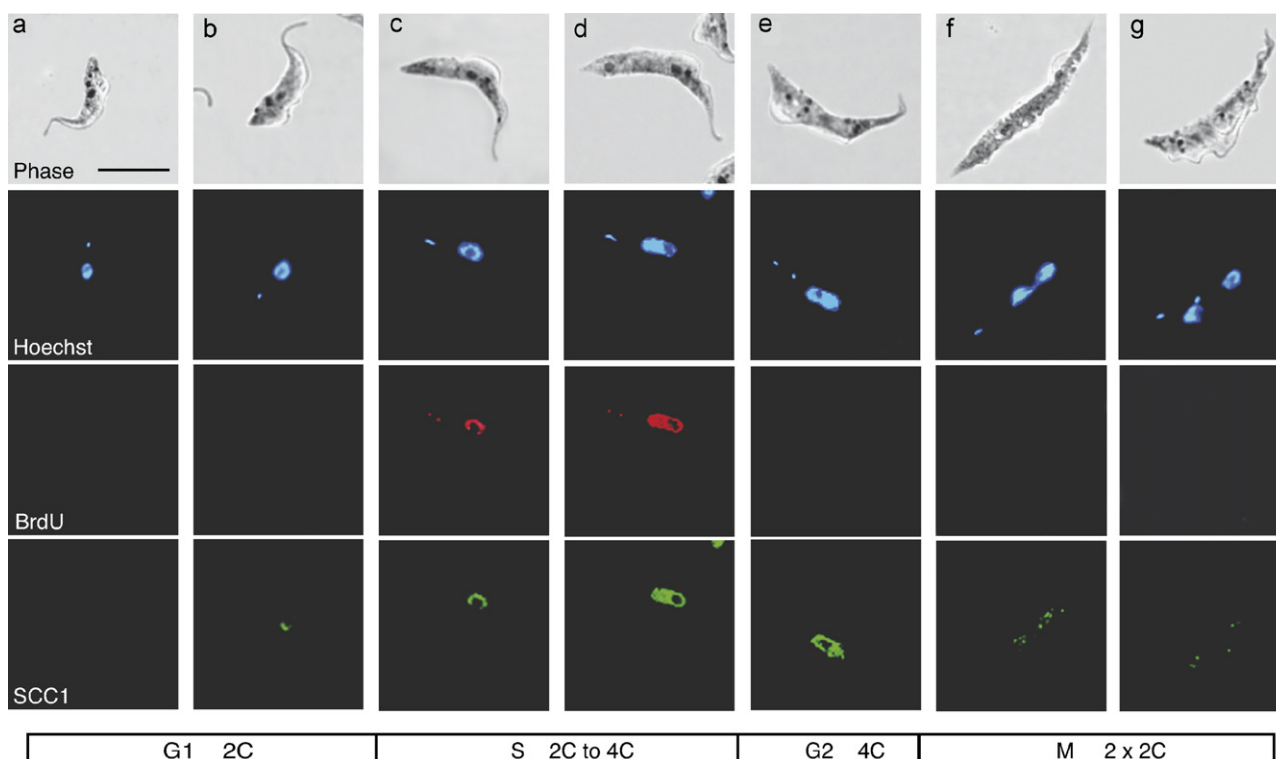
Figure 1. Expression profile of SCC1 during the course of the cell cycle in cultured procyclic form *Trypanosoma brucei*. In order to facilitate cell cycle staging, the cells were incubated with 5-bromo-2′-deoxyuridine (BrdU) and deoxycytidine for 2 h, fixed, and stained with anti-BrdU, anti-SCC1 and Hoechst 33258. Scale bar represents 10 μm.

4   R. Sharma et al.

Late G2 cells were 2K1N with two well separated kinetoplasts and had not incorporated BrdU (Fig. 1e); these cells were always SCC1 positive. Cells that were 2K2N had undergone nuclear division prior to cell division, these cells contained a few residual spots of SCC1 but were largely SCC1 negative (Fig. 1f and g). These results validated SCC1 as a marker for cell cycle stage in trypanosomes; S-phase and G2 cells were SCC1 positive and G1 and M phase cells were SCC1 negative.

Analysis of Procyclic Trypomastigotes from the Tsetse

One day after being taken up by a tsetse fly, bloodstream form trypanosomes have differentiated into proliferating procyclic trypomastigotes and have a range of kinetoplast and nucleus morphologies indicating that the cells are in various stages of the cell cycle from G1 to completion of mitosis (Fig. 2). The cells already exhibit the typical procyclic trypomastigote pattern of mitosis whereby one daughter kinetoplast is present between the divided nuclei (Fig. 2e) in contrast to the bloodstream trypomastigote pattern where the two daughter kinetoplasts are to the posterior side of both daughter nuclei. The presence or absence of SCC1 in cells with different karyotypes was similar to that for cultured procyclic cells; 16% cells were SCC1

negative and 84% were SCC1 positive. The combination of kinetoplast and nucleus morphology and presence or absence of SCC1 thus provided a method to determine cell cycle stage of trypanosomes isolated from tsetse flies. Attempts to label DNA by feeding flies with BrdU were unsuccessful.

After 2—3 days of infection, trypanosomes were found in the ectoperitrophic space and moved anteriorly in this compartment to colonise the proventriculus from 4 days onwards. During this time, trypanosomes continued to proliferate and elongated from 21.6 ± 0.9 (range 16—30) µm in the posterior midgut to 24.0 ± 1.5 (range 19—34) µm in the anterior midgut. The results showing the time course of an infection and the trypanosome cell types present in different parts of the fly are in Figures S2 and S3 in Supplementary Data. The proventriculus contained the largest range of trypanosome cell morphologies including all stages previously described from the foregut and proboscis (Lewis and Langridge 1947; Van den Abbeele et al. 1999). The remainder of the experiments concentrated on cells present in the proventriculus.

Cell Cycle Analysis of Trypanosomes from the Tsetse Proventriculus

Trypanosomes isolated from the proventriculus were stained for SCC1 to determine cell cycle
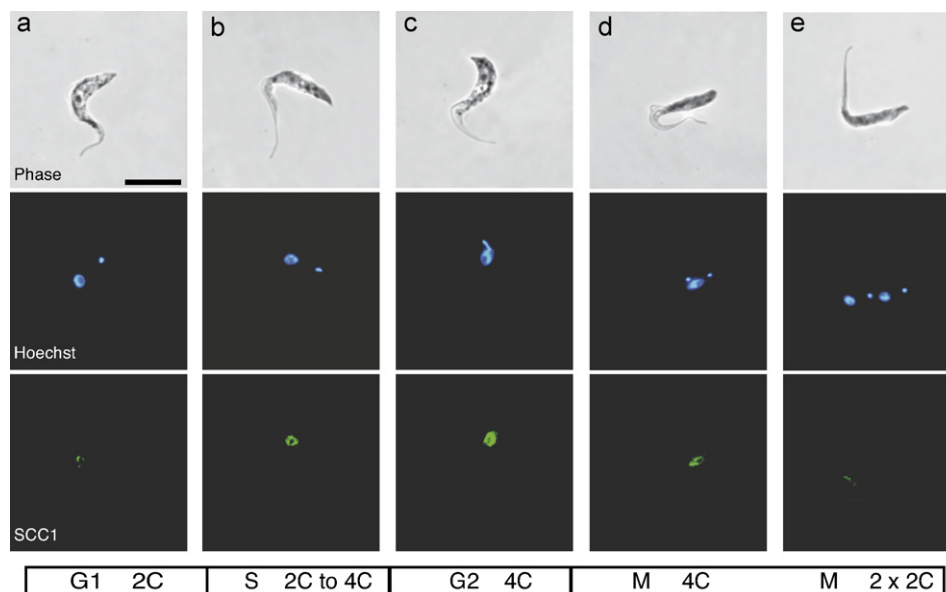
Figure 2. Procyclic trypomastigotes present in the midgut of tsetse flies on day 1 post-infection stained with Hoechst 33258 and anti-SCC1. Scale bar represents 10 µm.

stage and for DNA to determine the relative position of the nucleus and kinetoplast. The DNA staining and presence or absence of SCC1 enabled a sequential ordering of the various forms based on progression of morphological change, which included all the cell morphologies and staining patterns observed in trypanosomes isolated from the proventriculus. The ordering was based on: an increasing length of the cell, the progression from a round to elongated nucleus, the decreasing distance between the kinetoplast and the nucleus, the progression of the kinetoplast past the nucleus, the division of the kinetoplast, nucleus and cell, and the appearance and disappearance of SCC1. It became clear that all the observed cell types were from a single cell division cycle. The stages are described below and shown in Figure 3.

The elongation of the procyclic trypomastigotes that occurred during anterior migration in the midgut continued in the proventriculus and was accompanied by a change in the shape of the nucleus, first to an oval (Fig. 3a,b) and then an elongated form (Fig. 3c,d). During this progression SCC1 accumulated in the nucleus (Fig. 3a—d), indicating that the cells underwent S-phase during the elongation of the cell and nucleus. At the same time the average length of the cell increased from 24.0 ± 1.5 (range 19—34) μm in the anterior midgut to 35.1 ± 0.5 (range 30 to 38) μm (see Table S1 in Supplementary Data for measurements of cell dimensions). All trypomastigotes with an elongated nucleus were strongly SCC1 positive indicating that these cells were in S-phase or more probably G2 (see Fig. S4 in Supplementary Data for an analysis of SCC1 expression in
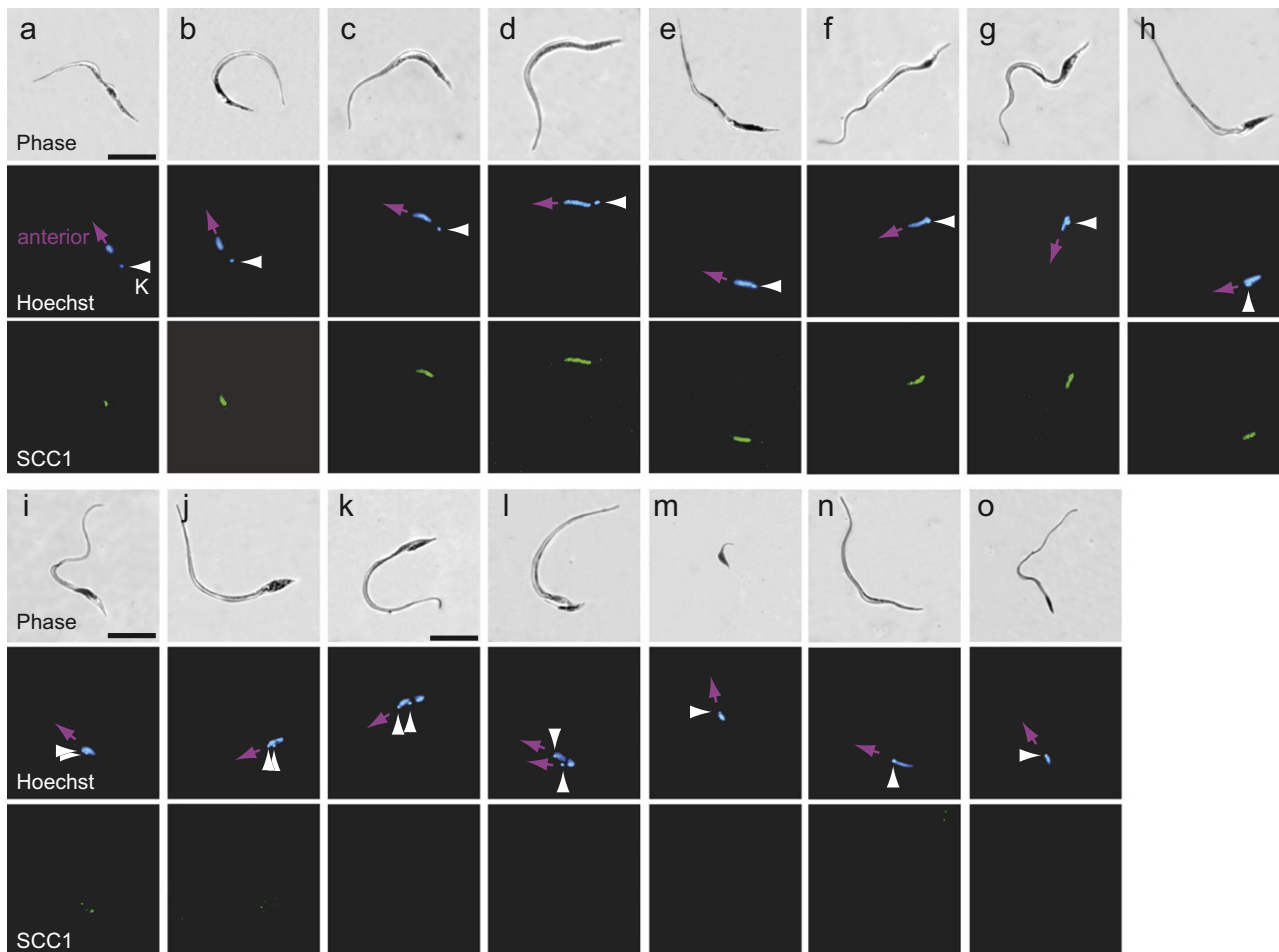
Figure 3. Trypanosome cell types found in the proventriculus and posterior oesophagus of tsetse flies stained with Hoechst 33258 and anti-SCC1. White arrows point to the kinetoplast and purple arrows to the anterior pole of the cell. The images are ordered to show the succession cell types leading up to and produced by a single asymmetric division. Scale bar represents 10 μm.

different cell types). No dividing trypomastigotes were observed. As the cells elongated, the distance between the nucleus and the kinetoplast reduced until the kinetoplast was in a juxta-nuclear position (Fig. 3c—e). The nucleus and kinetoplast then exchanged relative positions in the cell so that the kinetoplast which was previously posterior to the nucleus became anterior (Fig. 3f—j). First, the kinetoplast was in a posterior lateral juxta-nuclear position (Fig. 3f—g) and then in an anterior lateral juxta-nuclear position (Fig. 3h—i). Two other events coincided with relative movement of the kinetoplast from a posterior lateral to anterior lateral position: the kinetoplast divided (Fig. 3h—i) and the nucleus became SCC1-negative, indicating anaphase (Fig. 3i—j). At this stage the diameter of the posterior end of the cell was significantly larger that the anterior end. The cell then underwent nuclear division as an epimastigote (Fig. 3j—k) to form a 2K2N epimastigote that then underwent an asymmetric cell division (Fig. 3k—l) to produce one short (Fig. 3m) and one long (Fig. 3n) daughter epimastigote cell. The asymmetrical nature of the division is clear from the lengths of the two daughter cells: 9.3 $\pm$ 0.4 (range 7—13) μm and 32.4 $\pm$ 0.7 (range 24—37) μm. All the daughter epimastigote cells were SCC1-negative indicating that they remained in G1 whilst in the proventriculus. The fate of the long epimastigote remains unclear but they were often observed with diffuse staining of nuclear DNA (Fig. 3o) possibly indicating breakdown of the nucleus. The short epimastigote was similar to unattached epimastigotes found in the salivary glands.

The seven cell morphologies from the proventriculus described above were present from day 5 onwards during an infection and the proportions of different cell types present in proventriculi did not vary greatly over time (Fig. S5 in Supplementary Data). Thus, the differentiation to epimastigotes occurred shortly after the proventriculus was colonised and continued throughout the infection. In addition, the absence from the proventriculus of both dividing trypomastigotes and SCC1-positive epimastigotes suggested that the proventricular trypanosome population is not self-sustaining and requires the continuous arrival of new trypomastigotes from the midgut.

Expression of Procyclins

Procyclins are the dominant macromolecule present on the surface of procyclic trypomastigotes. Cells isolated form the midgut and proventriculus were stained for GPEET and EP procyclin (Fig. 4). Midgut procyclic trypomastigotes isolated early in an infection (days 1—3) predominantly expressed GPEET procyclin with EP procyclin in some cells (Fig. 4a—c). In the proventriculus, trypomastigotes expressed EP procyclin (Fig. 4d,e) but the EP procyclin began to diminish as the asymmetric cell division started with the movement of the kinetoplast and nucleus relative to each other (Fig. 4f,g). The short epimastigote daughter cell did not express EP procyclin (Fig. 4i) and there was very limited expression in long epimastigotes (Fig. 4h). The gradual loss of EP procyclin during the later stages of the asymmetric cell division cycle supported the ordering of cell morphologies above. No cell in the salivary glands was positive for either type of procyclin (data not shown).

Morphometry of the Proventricular Cell Cycle

Cell dimensions were derived from both phase microscopy images and the location of the nucleus and kinetoplast within the cell by combining fluorescence images of Hoechst-stained cells with phase overlays (Table S1 in Supplementary Data). The extension of the flagellum beyond the cell body was measured from scanning electron microscope images. In trypomastigotes the extension of the flagellum beyond the cell body constituted 14—23% of the total cell length (average, 18%; $n = 11$). The percentage appeared to be independent of total cell length. The changes in cell dimensions and location of the nucleus and kinetoplast are shown in a diagrammatic form Figure 5. The most striking observation from this analysis is that the distance between the kinetoplast and the posterior pole of the cell is relatively constant (Fig. 5, green to purple lines) whereas the distance between the nucleus and the posterior pole (green to yellow lines) is greatly reduced during the transition from trypomastigote to epimastigote. The second observation is that the distortion of the shape of the nucleus to an elongated form of aspect ratio 5:1 during the asymmetric cell division is coincident with the elongation and narrowing of the whole cell and the subsequent cell diameter (1.2 μm) is less than the original diameter of the spherical nucleus (1.6 μm).
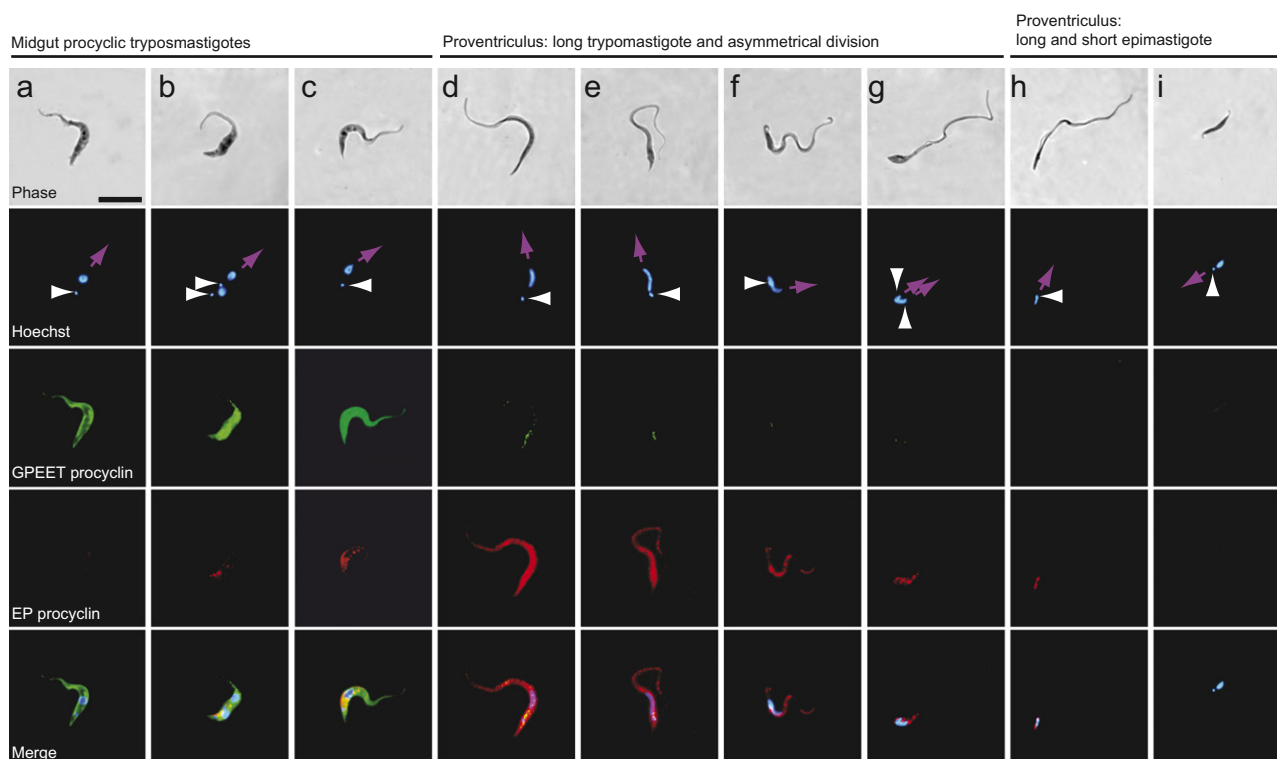
Figure 4. Trypanosome cell types from the midgut and proventriculus of tsetse flies stained with Hoechst 33258, anti-GPEET procyclin and anti-EP procyclin. The midgut procyclic trypomastigotes were collected between day 1 and day 4 of infection. White arrows point to the kinetoplast and purple arrows to the anterior pole of the cell. Scale bar represents 10 μm.

Electron Microscopy of the Asymmetric Division

Scanning and transmission electron microscopy were used to provide a more detailed view of the cell morphologies during the asymmetric cell division cycle. Fig. 6a illustrates the large asymmetry in the dividing cell. The old flagellum is extremely long (~35 μm) and overhangs the anterior end of the cell. The posterior end of the cell shows the characteristic broadening and the short new flagellum has extended such that its tip is closely associated with the old flagellum. Figure 6b—e shows progression of an asymmetric division. At an early stage, the very short new flagellum and the old flagellum are emerging from the same flagellar pocket (Fig. 6b). The new flagellum then lengthens and the distance between the two flagellar pockets increases (Fig. 6c—e). The tip of the new flagellum remains associated with the lateral aspect of the old flagellum, suggesting the presence of a flagella connector (Fig. 6c—e). As the new flagellum
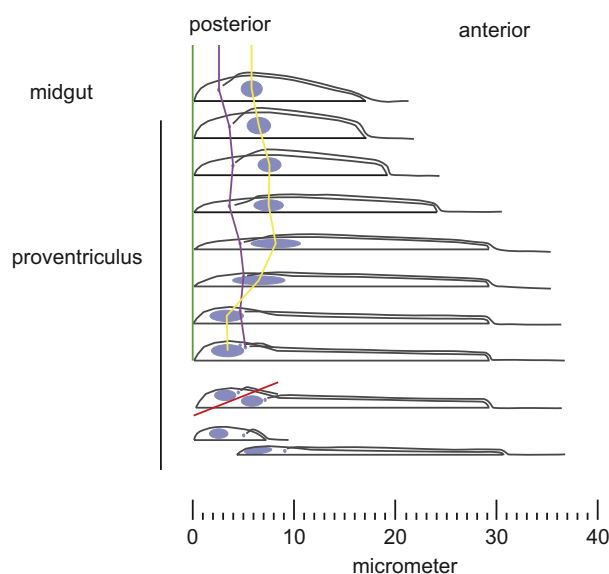
Figure 5. Diagram representing the changes in cell dimensions and location of organelles during the cell cycle that ends with the asymmetric division and the production of epimastigotes.

8   R. Sharma et al.
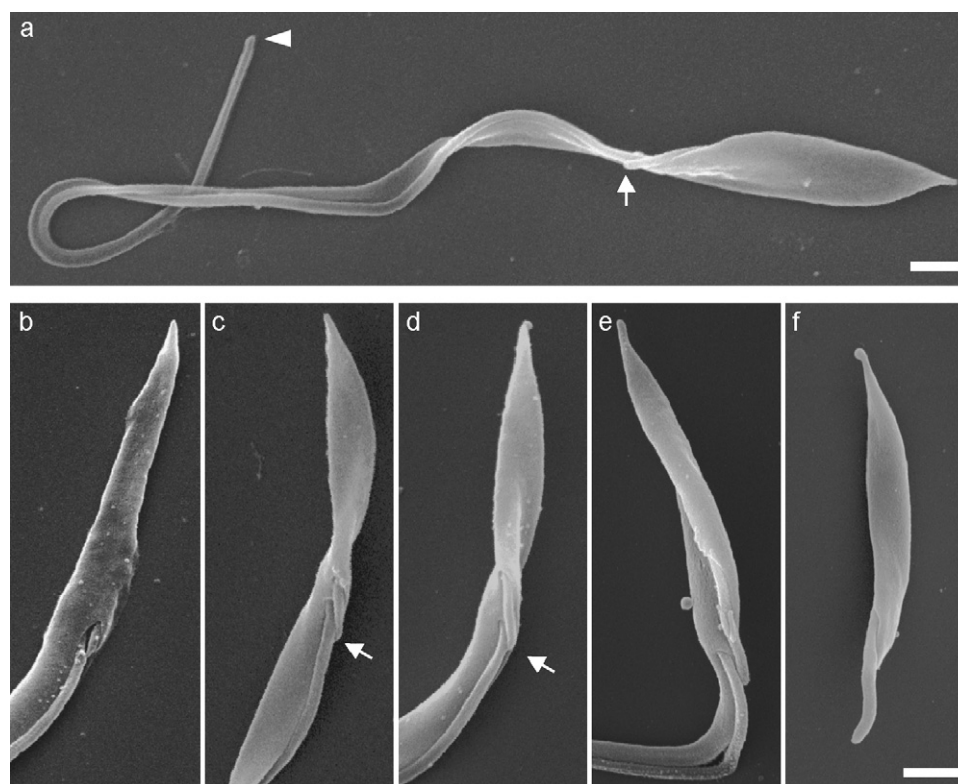
Figure 6. Progression of the asymmetric division viewed by scanning electron microscopy. (a) View of a whole cell with a long old flagellum (tip marked with an arrowhead) and a short new flagellum (tip marked with an arrow). (b—e) Successive stages of the division process. The cell in b is at an early stage, with the tip of the new flagellum just emerging from the flagellar pocket. As the new flagellum elongates, its tip (arrow) remains associated with the old flagellum, indicative of the presence of a flagella connector. In E the new flagellum has reached its maximal length and the cleavage fold is apparent. (f) Post-division small epimastigote. Scale bars represent 1 μm.

reaches its maximal length, a cleavage fold is very apparent (Fig. 6e). Figure 6f shows the smaller post-division epimastigote.

Transmission electron micrographs of elongated trypanosomes with the kinetoplast close to the nucleus showed that the diameter of the nucleus was not much less that that of the cell with little cytoplasm between the nuclear and plasma membranes (Fig. 7a,b), and revealed the juxtaposition of the nucleus and flagellar pocket as one passed the other (Fig. 7b). The distance between the subpellicular microtubules is normal (Fig. 7a and c). A section through an asymmetrically dividing cell shows a flagella connector-like structure (Briggs et al. 2004; Moreira-Leite et al. 2001) at the tip of the new flagellum (Fig. 7c). No examples of kinetoplasts that were not juxtaposed to a basal body were found and, by light microscopy, kinetoplasts were always positioned at the proximal end of the flagellum. Taken together these observations indicate that the

kinetoplast and basal body segregation were coupled as in other life cycle stages. In the electron micrographs, there was no indication that the flagella were disconnected from the cell body except for the anterior extension and a flagellum attachment zone structure was observed wherever the flagellum ran along the cell body.

Epimastigotes in the Salivary Gland are SCC1-Positive

The observation that epimastigotes from the proventriculus were always SCC1-negative indicated that they are in G1. In contrast, populations of epimastigotes isolated from the salivary glands contained a percentage of SCC1-positive cells (Fig. 8). The epimastigotes could be divided into two types, those free in the salivary gland ducts and those attached to the epithelium. In the
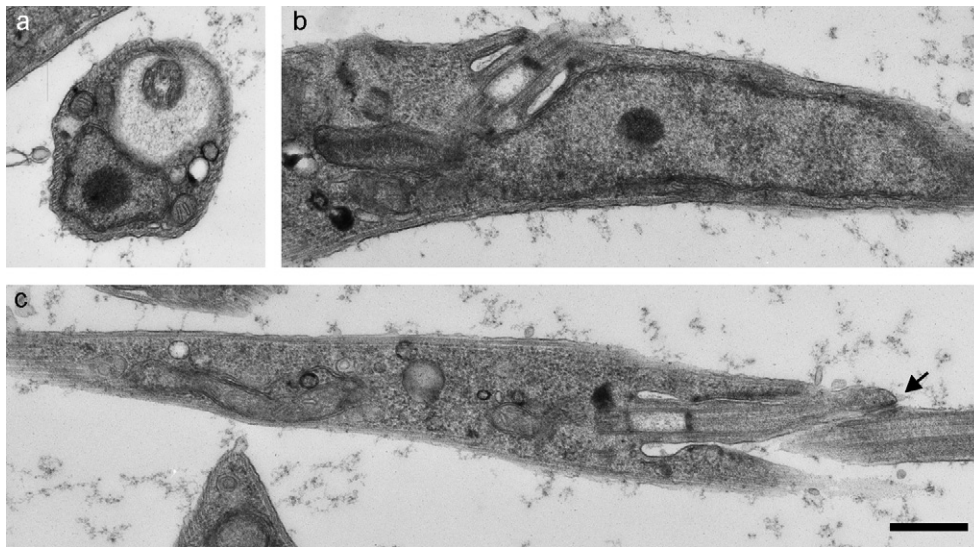
Figure 7. Thin section electron micrographs of proventricular trypanosomes. (a—b) In elongated cells the nucleus is in close proximity to the plasma membrane, and the juxtaposition of flagellar pocket and nucleus are visible. (c) Posterior end of an asymmetrically dividing cell, showing a new flagellum emerging from the flagellar pocket. The tip of the new flagellum is connected to the old flagellum (arrow). Scale bar represents 500 nm.
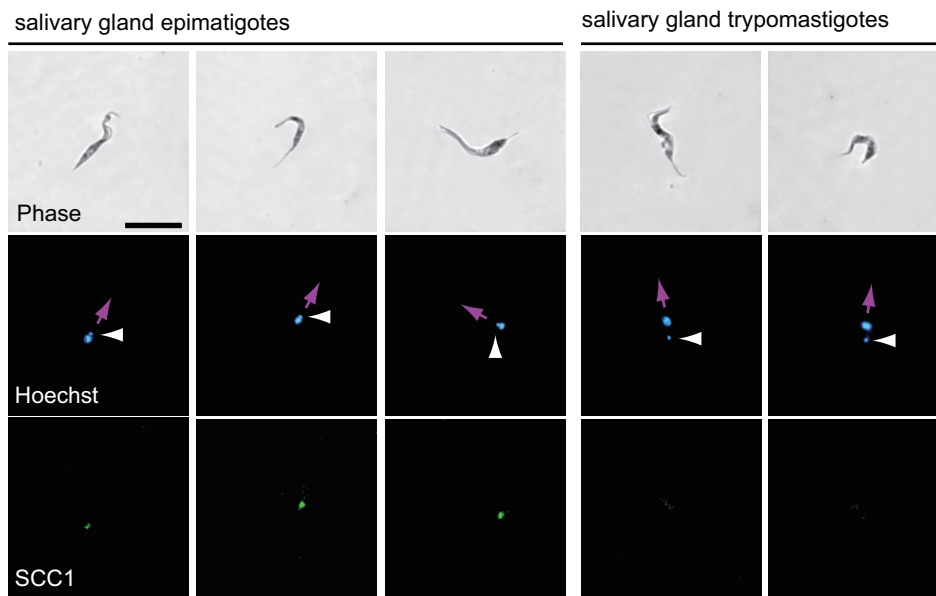
Figure 8. Trypanosome cell types found in the salivary glands of tsetse flies stained with Hoechst 33258 and anti-SCC1. White arrows point to the kinetoplast and purple arrows to the anterior pole of the cell. Scale bar represents 10 μm.

unattached population, 35% were SCC1-positive whereas 90% of the attached epimastigotes were SCC1-positive (Fig. S2 in Supplementary Data). These observations are consistent with short epimastigotes being arrested in G1 in the proven-

triculus and starting to proliferate once in the salivary glands, and possibly proliferation being stimulated by attachment. The volume of the attached epimastigotes present in the salivary gland was at least double that of the short

epimastigotes present in the proventriculus (cellular dimensions are in Table S1 in Supplementary Data). It is possible that this growth is a requirement for the cells to enter S-phase but it is not easily determined whether the growth occurs during transit, once the epimastigote has arrived in the salivary gland or after attachment.

Scanning Electron Microscopy of Proventricular and Salivary Gland Stages

An overview of the cell morphologies found in the proventriculus is shown in Figure 9a—d. The predominant proventricular trypomastigotes are elongated cells with a single flagellum (Fig. 9a). Frequently, a bead-like structure was present at the anterior end of the cell body (Fig. 9a inset), the nature and significance of this structure is unknown. Dividing cells are highly asymmetric, with a very short new flagellum attached via its tip to the old flagellum (Fig. 9b). The small epimastigote daughter cells that are a product of the asymmetric division have a short flagellum (Fig. 9c—d) and frequently a characteristic protrusion at the posterior end of the cell (Fig. 9d). In the salivary gland, epimastigotes are attached to the epithelium via their flagellum, and these cells possess a long posterior protrusion (Fig. 9e). Metacyclic trypomastigotes are unattached and the posterior end of the cell assumes a blunt appearance (Fig. 9f).
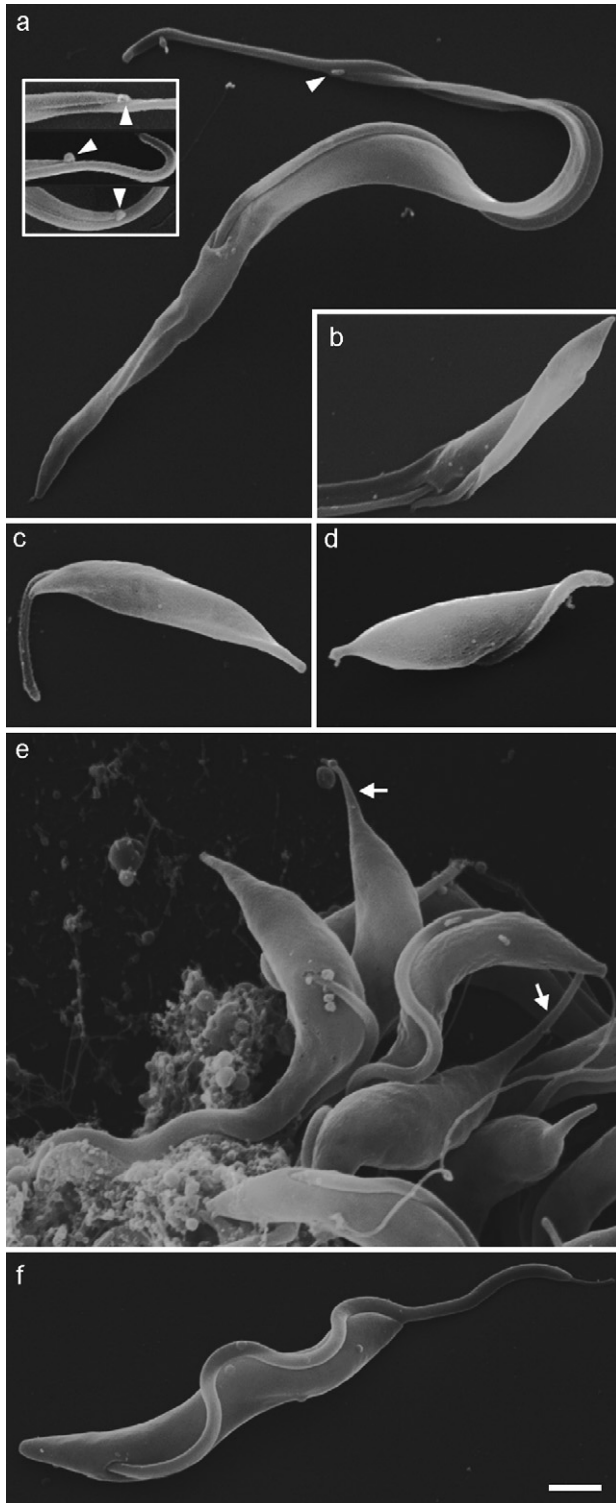
Discussion

There are at least five changes in cellular morphology during the life cycle of *Trypanosoma brucei* and only one of these, the differentiation from bloodstream trypomastigote to procyclic trypomastigote, has been investigated in detail. In this paper, the transition from procyclic trypomastigote to salivary gland epimastigote has been investigated. This differentiation involves a

Figure 9. Scanning electron micrographs illustrating different trypanosome forms found in the tsetse proventriculus and salivary glands. (a) Long trypomastigote. A bead-like structure of unknown nature that is frequently observed at the anterior tip of the cell body is marked by an arrowhead; the inset shows further examples. (b) Posterior end of an asymmetrically dividing cell with a clearly visible cleavage fold. (c—d) Short epimastigotes found in the proventriculus. (e) Epimastigotes in the salivary gland are attached to the gland epithelium via their flagellum. Long protrusions extending from the posterior end of the epimastigote cells are marked with arrows. (f) Metacyclic trypomastigote. Scale bar represents 1 μm.

reduction in cell length, an exchange in relative positions of the nucleus and kinetoplast along the anterior posterior axis of the cell, that is from a trypomastigote to an epimastigote cellular morphology, and the loss of the predominant procyclic cell surface macromolecule. In contrast to the differentiation of bloodstream form to procyclic trypomastigotes which occurs during a G1 arrest, the differentiation of trypomastigotes to epimastigotes occurs during an asymmetric cell division cycle. The reduction in cell length is achieved by an asymmetric cell division and apparent sacrifice of the longer daughter cell. The rearrangement of the nucleus and kinetoplast results from a relative movement of the nucleus towards the posterior of the cell and occurs at the same time as the nuclear division that precedes the asymmetric cell division. The loss of the EP procyclin from the cell surface occurs around the time of the cell division.

The description of the asymmetric cell division cycle here is largely in agreement with earlier reports that proventricular trypomastigotes differentiate to epimastigotes via an asymmetric division (Lewis and Langridge 1947; Van den Abbeele et al. 1999). The most comprehensive description (Van den Abbeele et al. 1999) used measurements of DNA content to show that procyclic trypomastigotes arrive at the proventriculus in G1 arrest (2C), undergo S-phase and on completion differentiate into long epimastigotes whilst in G2 (4C) before undergoing an asymmetric division to produce one short and one long daughter epimastigote. The details we have been able to add through the use of SCC1 as a cell cycle marker, analysis of procyclin expression and more detailed visualization of morphology are: (1) the gross change in nuclear morphology occurs during S-phase of the asymmetric cell division cycle. (2) The exchange in relative positions of the nucleus and kinetoplast on the anterior posterior axis of the cell occurs during mitosis in the asymmetric cell division cycle and anaphase occurs before the kinetoplast is to the anterior side of the nucleus. Prior to mitosis the trypomastigote is a 1K1N cell in G2, whereas the kinetoplast divides during the first half of G2 in procyclic trypomastigotes (Woodward and Gull 1990) resulting in most G2 cells being 2K1N. (3) The division of the kinetoplast is co-incident with nuclear anaphase and occurs whilst the kinetoplast is laterally disposed to the nucleus. (4) No SCC1-positive epimastigotes were observed in the proventriculus. (5) The new flagellum emerges from the same flagellar pocket as the old flagellum and the tip of the new flagellum appears to be attached to the old flagellum via a structure similar to the flagella connector (Briggs et al. 2004; Moreira-Leite et al. 2001). (6) The exchange of the relative positions of the kinetoplast and nucleus is primarily a result of a reduction in the distance between the nucleus and the posterior of the cell, the distance between the posterior and kinetoplast is relatively constant. (7) EP procyclin, the most abundant cell surface macromolecule (Roditi et al. 1987), is lost from the cell surface during the asymmetric cell division cycle. (8) The long epimastigote daughter cell does not enter S-phase as judged by the lack of expression of SCC1 and it is likely that the cell degenerates as many were observed with diffuse or dispersed nuclear staining.

The changes in cell morphology described above involved a gradual elongation of a cell followed by a dramatic shortening via an asymmetric division. The cellular shape of a trypanosome is defined by a helical corset of microtubules and elongation during proliferative growth of procyclic trypomastigotes is achieved by sliding of microtubules against one another, insertion of new short microtubules and by the elongation of microtubules, primarily at the posterior end of the cell (Robinson et al. 1995). The progressive elongation of midgut trypomastigote forms, from 21 to 36 µm by the time the asymmetric cell division is initiated, probably occurs by the same mechanism. The alternative mechanism involving twisting the spiral corset to elongate the cell would likely involve alterations in the spacing between microtubules and a very different helical pitch. However, the distance between microtubules remained the same in transmission electron micrographs of all cell types from the proventriculus. How does the trypanosome reverse an elongation in cell form given the stability of the microtubule corset? The asymmetric division achieves a shortening in length from 21 µm in the procyclic trypomastigote to 9 µm for the short epimastigote with maintenance of the microtubule corset. There is a second shortening in cell length during the life cycle during the differentiation of 'long slender' to 'short stumpy' bloodstream form trypomastigotes (Vassella et al. 1997; Vickerman 1985). However, this change in form also includes an increase in cell diameter and it is not clear whether it is a result of an asymmetric division producing a shorter daughter cell or results from sliding of microtubules in the corset.

Initiation of growth of the new flagellum is one of the earliest events in the cell division cycle in procyclic trypomastigotes (Sherwin and Gull 1989a). As the cell cycle progresses, the new

12   R. Sharma et al.

flagellum extends to about half of the length of the old flagellum, to which it remains attached via the flagella connector (Moreira-Leite et al. 2001). At that point, there is a rapid increase in the distance between basal bodies and separation of daughter kinetoplasts (Davidge et al. 2006). The basal bodies are directly connected to the kinetoplasts and the separation of basal bodies can be visualised as separation of the two daughter kinetoplasts (Ogbadoyi et al. 2003). In procyclic trypomastigotes, the daughter kinetoplasts separate during early G2 (Robinson and Gull 1991). Initially the new flagellum emerges through the same flagellar pocket as the old flagellum and subsequently the flagellar pocket divides so that each contains a single flagellum (Moreira-Leite et al. 2001). The length of the new flagellum has a profound effect on the location of the cleavage in the subsequent cell division. In procyclic cells the new flagellum can be made shorter than usual by inhibiting intraflagellar transport using RNAi and the subsequent site of initiation of cleavage is altered with the result that there is an asymmetric division (Kohl et al. 2003). One of the most notable features of the asymmetric division that occurs in the proventriculus is the disparity in length of the new and old flagellum. The behaviour of the new flagellum is similar to that in procyclic cells; it emerges from the same pocket as the old flagellum and the tip remains attached to the old flagellum, probably via a flagella connector. The restricted length of the new flagellum could provide the spatial information that positions the asymmetric division plane.

By the time that mitosis and cytokinesis occurs in proliferating procyclic trypomastigotes the new flagellum is almost as long as the old flagellum (Robinson et al. 1995) and there is only limited growth of the new flagellum in the daughter cell. In all proventricular stages measured, the flagellum extended beyond the anterior pole of the cell by 15—20% of the total flagellum length. During the asymmetric cell division cycle the trypanosome elongates by 6 μm between the onset of S-phase and cell division, this is accompanied by continuous elongation of the flagellum throughout the cell cycle, so the elongation of the cell body is accompanied by a proportional growth in the flagellum. The flagella of many unicellular organisms, such as *Chlamydomonas reinhardtii*, are ephemeral and are reabsorbed at cell division and can also vary in length depending on parameters such as component availability. In other species, such as trypanosomes, the flagella is maintained throughout the cell cycle and the usual situation is

either possession, or not, of a flagellum of a defined length. Hence, this demonstration of the ability of a trypanosome to control the length of its flagellum, first in the production of a long flagellum in the progenitor cell and second in the formation of the short flagellum in the asymmetric division, defines a new level of flagellum length control hitherto unreported.

Once in the salivary glands the epimastigotes attach to the gland epithelium via an elaborated flagellum membrane (Vickerman et al. 1988). The attached epimastigotes proliferate whilst remaining attached to the epithelium (Vickerman et al. 1988). The repositioning of the basal body to the anterior half of the cell, nearer to the origin of cell division cleavage, may facilitate cytokinesis in trypanosomes attached to a substratum through the flagellum. Other kinetoplastids that attach to epithelia in their hosts, such as the promastigotes of *Leishmania* spp., epimastigotes in other trypanosome species and the insect-infecting *Crithidia* species, also have basal bodies in the anterior part of the cell. In contrast, there are no reported examples of trypomastigotes that proliferate whilst attached. It is a puzzle why trypanosomes rearrange the position of their organelles and anterior positioning of the basal body may be necessary to allow division of kinetoplastid cells attached by a flagellum.

The loss of EP procyclin during the asymmetric cell division cycle was not unexpected as it has been reported that the protein is absent in salivary glands (Urwyler et al. 2005) and more recently it has been shown that the predominant proteins on the surface of epimastigote forms are a family of alanine rich proteins previously known as BARP (Urwyler et al. 2007). The high level of expression of procyclins is an adaptation to the tsetse midgut, the epimastigote is adapted for migration to and colonisation of the salivary glands. It would be interesting to know whether the composition of the membrane on the new flagellum was the same as the old or included additional proteins necessary for the membrane elaboration and attachment that occurs in the salivary glands (Vickerman et al. 1988).

Some unexpected observations were made using scanning electron microscopy of whole cells. The elongated trypomastigotes had a discrete bead-like structure at the anterior end of the cell body (Fig. 9a) and the attached epimastigotes had a spike-like protrusion at the posterior end, both in the proventriculus (Fig. 9c,d) and, in a more exaggerated form, facing away from the epithelium in the salivary gland (Tetley and

Vickerman 1985) (Fig. 9e). Both these structures remain of unknown function but it is tempting to speculate that the protrusion in the epimastigote, which exposes a greater surface area of plasma membrane to the gland lumen, may be involved in some interaction with signal from or to the environment.

Here, we have provided a more detailed description of an asymmetrical cell division cycle that is an integral part of the *Trypanosoma brucei* life cycle. The cell cycle includes an exquisitely synchronised exchange in organelle location along the anterior posterior axis and asymmetric division that are coupled to a change in cell surface architecture. The behaviour of the new flagellum is consistent with a role in determining the location of the plane of cell division, previously characterised in procyclic cells. The asymmetric division may represent a mechanism to produce a large reduction in cell length in a cell shaped by a stable microtubule array. It now remains to determine how the changes in cell morphology are reversed when the epimastigote differentiates back to a trypomastigote in the salivary glands.

Methods

Trypanosomes: Procyclic forms of *Trypanosoma brucei brucei* Lister 427 were cultured in SDM-79 medium (Brun and Schönenberger 1979). Male tsetse flies, *Glossina morsitans morsitans*, were infected 24—48 h post-eclosion with bloodstream form *T. b. brucei* J10 (MCRO/ZM/74/J10 [clone 1]) in sterile defibrinated horse blood containing 60 mM N-acetyl glucosamine and 4×10^6 trypanosomes/ml. Maintenance feeding of flies was on sterile horse blood.

Dissection: Flies were starved for 48 h before dissection where possible to avoid contamination with blood. Whole tsetse alimentary tracts, from the proventriculus to the rectum, were dissected in a drop of PBS (137 mM sodium chloride, 2.7 mM potassium chloride, 10.1 mM di-sodium hydrogen phosphate, 1.8 mM potassium di-hydrogen phosphate pH 7.6) at various time points during the course of the infection; daily from day 1 to day 10 post infection, and subsequently every alternate day until day 28 or day 35 depending on the experiment. Sections of the gut (proventriculus and posterior oesophagus, anterior midgut, posterior midgut) and salivary glands were placed separately in 50 μl drops of PBS on polylysine coated slides. The various gut segments were teased apart with 26 gauge needles to release the trypanosomes. The trypanosomes were fixed in 2% paraformaldehyde and processed for immunofluorescence microscopy. To collect migratory forms from the oesophagus and mouthparts, flies were allowed to probe onto warm, alcohol-cleaned microscope slides prior to feeding, having received their last meal 48 h previously (Lewis and Langridge 1947). The dried drops of salivary exudate were rehydrated by immersing the slides in PBS as soon as possible and then processed as above.

Production of anti-SCC1: The gene Tb927.7.6900 (http://www.genedb.org/genedb/tryp/) was identified as a putative orthologue of SCC1 using BLAST searches. The open reading frame was amplified using the oligonucleotides: 5′-AAG-CTTCCGCCACCATGTTCTACTCAACCTAC and 5′-TGATCAA-GAACCCACAGTGAGTTGCACCTC. The subsequent HindIII BclI fragment was cloned into the HindIII and BclI sites of p2171, a derivative of pET15b. The recombinant SCC1 was expressed in *E. coli* BL21 (DE3) and was insoluble. It was purified by preparative SDS-PAGE and used to immunise one rabbit. The anti-SCC1 was affinity purified using Western blot strips containing recombinant SCC1.

Light microscopy: Cultured procyclic form trypanosomes were washed with vPBS (137 mM sodium chloride, 2.7 mM potassium chloride, 16 mM sodium phosphate 3 mM potassium di-hydrogen phosphate, 46 mM sucrose, 10 mM glucose, pH 7.6) and were fixed in an equal volume of 4% paraformaldehyde in PBS for 15 min on ice. Nonidet NP-40 was added to a final concentration of 0.1% and the cells incubated at room temperature for 10 min. The cells were allowed to settle on polylysine-coated slides for 15 min in a humid chamber. Slides were washed as follows: 2×5 min in PBS, 2×5 min in 0.5 M glycine, 2×5 min in PBS, then incubated for an hour with blocking solution (10% normal donkey serum in PBS) in a humid chamber. Slides were incubated with affinity purified primary antibody in blocking solution for 1 hour at room temperature, then washed for 3×5 min in PBS. Slides were incubated with Alexafluor 488-conjugated donkey anti-rabbit or Alexafluor 594-conjugated donkey anti-mouse secondary antibodies diluted 1:200 in blocking solution for 1 h at room temperature, then washed 3×5 min in PBS. Following the last wash, slides were incubated with 0.1 μg/ml Hoechst 33258 in PBS for 15 min. The slides were mounted using FluorSave reagent, dried overnight at 15 °C and stored at 4 °C. The following primary antibodies were used for immunofluorescence analyses: Rabbit anti-SCC1; anti-EP procyclin monoclonal (a kind gift of Terry Pearson); rabbit anti-GPEET polyclonal (a kind gift of Terry Pearson). Slides were viewed using a Nikon Optiphot-2 epifluorescence microscope with the appropriate filters. Digital raw grey images (8 bit and 16 bit) were taken with an attached digital camera (Photometrics Coolsnap *fx*), using a $100 \times$ objective (Nikon Plan 1.25na oil) and RS Image version 1.0.1 software (Roper Scientific, Inc). Images were later imported into Adobe Photoshop CS and false colour was added using the channel mixer tool. Final images were assembled in Adobe Illustrator CS.

Cell morphometry: Digital measurements were performed on individual cells using the morphometry software ImageJ (Research Services Branch, National Institutes of Health, Bethesda, Maryland, USA). All measurements were μm and reported as the mean $\pm$ s.e. and ranges.

BrdU labelling: Bromo-2-deoxyuridine and deoxycytidine were added to a final concentration of 50 μM to a culture of procyclic trypanosomes in SDM-79. After two hours the cells were harvested, fixed as above, and the incorporated BrdU visualised using an anti-BrdU and endonuclease cocktail (GEC/Amersham) according to the manufacturers instructions.

Electron microscopy: For scanning electron microscopy, the proventriculus and salivary glands were dissected on polylysine coated coverslips and trypanosomes were left to settle for at least 5 min. The cells were then fixed with 2.5% glutaraldehyde in 100 mM phosphate buffer pH 7.4 overnight, washed with water, and dehydrated through an ethanol series. The coverslips were critical-point dried and coated with gold.

14   R. Sharma et al.

For thin section transmission electron microscopy, the proventriculus was placed directly in 2.5% glutaraldehyde, 2% paraformaldehyde and 0.1% picric acid in 100 mM phosphate (pH 7.2) and processed as described previously (Dawe et al. 2005).

Acknowledgements

Appendix A. Supplementary materials

The supplementary data associated with this article can be found in the online version at doi:10.1016/j.protis.2007.07.004

References

Aksoy S, Gibson W, Lehane MJ (2003) Interactions between tsetse and trypanosomes with implications for the control of trypanosomiasis. Adv Parasitol **53**: 1—83

Angelopoulos E (1970) Pellicular microtubules in the family Trypanosomatidae. J Protozool **17**: 39—51

Briggs LJ, McKean PG, Baines A, Moreira-Leite F, Davidge J, Vaughan S, Gull K (2004) The flagella connector of *Trypanosoma brucei*: an unusual mobile transmembrane junction. J Cell Sci **117**: 1641—1651

Brun R, Schönenberger M (1979) Cultivation and *in vitro* cloning of procyclic culture forms of *T. brucei* in a semi-defined medium. Acta Tropica **36**: 289—292

Davidge JA, Chambers E, Dickinson HA, Towers K, Ginger ML, McKean PG, Gull K (2006) Trypanosome IFT mutants provide insight into the motor location for mobility of the flagella connector and flagellar membrane formation. J Cell Sci **119**: 3935—3943

Dawe HR, Farr H, Portman N, Shaw MK, Gull K (2005) The Parkin co-regulated gene product, PACRG, is an evolutionarily conserved axonemal protein that functions in outer-doublet microtubule morphogenesis. J Cell Sci **118**: 5421—5430

Hemphill A, Lawson D, Seebeck T (1991) The cytoskeletal architecture of *Trypanosoma brucei*. J Parasitol **77**: 603—612

Hoare CA, Wallace FG (1966) Developmental stages of trypanosomatid flagellates: a new terminology. Nature **212**: 1385—1386

Kohl L, Robinson DR, Bastin P (2003) Novel roles for the flagellum in cell morphogenesis and cytokinesis in trypanosomes. EMBO J **22**: 5336—5346

Lengronne A, McIntyre J, Katou Y, Kanoh Y, Hopfner KP, Shirahige K, Uhlmann F (2006) Establishment of sister chromatid cohesion at the *S. cerevisiae* replication fork. Mol Cell **23**: 787—799

Lewis EA, Langridge WP (1947) Developmental forms of *Trypanosoma brucei* in the saliva of *Glossina pallipedes* and Glossina austeni. Ann Trop Med Parasitol **41**: 6—13

Matthews KR (2005) The developmental cell biology of *Trypanosoma brucei*. J Cell Sci **118**: 283—290

Matthews KR, Sherwin T, Gull K (1995) Mitochondrial genome repositioning during the differentiation of the African trypanosome between life cycle forms is microtubule mediated. J Cell Sci **108**: 2231—2239

Moreira-Leite F, Sherwin T, Kohl L, Gull K (2001) A trypanosome structure involved in transmitting cytoplasmic information during cell division. Science **294**: 610—612

Nasmyth K (2005) How might cohesin hold sister chromatids together? Philos Trans R Soc Lond B Biol Sci **360**: 483—496

Ogbadoyi EO, Robinson DR, Gull K (2003) A high-order trans-membrane structural linkage is responsible for mito-chondrial genome positioning and segregation by flagellar basal bodies in trypanosomes. Mol Biol Cell **14**: 1769—1779

Robinson DR, Gull K (1991) Basal body movements as a mechanism for mitochondrial genome segregation in the trypanosome cell cycle. Nature **352**: 731—733

Robinson DR, Sherwin T, Ploubidou A, Byard EH, Gull K (1995) Microtubule polarity and dynamics in the control of organelle positioning, segregation, and cytokinesis in the trypanosome cell cycle. J Cell Biol **128**: 1163—1172

Roditi I, Carrington M, Turner M (1987) Expression of a polypeptide containing a dipeptide repeat is confined to the insect stage of *Trypanosoma brucei*. Nature **325**: 272—274

Roditi I, Schwartzm H, Pearson TW, Beecroft RP, Liu MK, Richardson JP, Bühring H-J, Pleiss J, Bülow R, Williams RO, Overath P (1989) Procyclin gene expression and loss of the variant surface glycoprotein during differentiation of *Trypanosoma brucei*. J Cell Biol **108**: 737—746

Sherwin T, Gull K (1989a) The cell division cycle of *Trypanosoma brucei brucei*: timing of event markers and cytoskeletal modulations. Philos Trans R Soc Lond B Biol Sci **323**: 573—588

Sherwin T, Gull K (1989b) Visualization of detyrosinylation along a single microtubule reveals novel mechanisms of assembly during cytoskeletal duplication in trypanosomes. Cell **57**: 211—221

Szoor B, Wilson J, McElhinney H, Tabernero L, Matthews KR (2006) Protein tyrosine phosphatse *Tb*PTP1: a molecular switch controlling life cycle differentiation in trypanosomes. J Cell Biol **175**: 293—303

Tetley L, Vickerman K (1985) Differentiation in *Trypanosoma brucei*: host—parasite cell junctions and their persistence during during acquisition of the variable antigen coat. J Cell Sci **87**: 363—372

Tetley L, Turner CMR, Barry JD, Crowe JS, Vickerman K (1987) Onset of expression of the variant surface glycoproteins of *Trypanosoma brucei* in the tsetse fly studied using electron microscopy. J Cell Sci **87**: 363—372

Tyler KM, Matthews KR, Gull K (2001) Anisomorphic cell division by African trypanosomes. Protist **152**: 367—378

Uhlmann F, Lottspeich F, Nasmyth K (1999) Sister-chromatid separation at anaphase onset is promoted by cleavage of the cohesin subunit Scc1. Nature **400**: 37—42

Urwyler S, Studer E, Kunz Renggli C, Roditi I (2007) A family of stage-specific alanine-rich proteins on the surface of epimastigote forms of *Trypanosoma brucei*. Mol Microbiol **63**: 218—228

Urwyler S, Vassella E, Van den Abbeele J, Renggli CK, Blundell PA, Barry JD, Roditi I (2005) Expression of procyclin mRNAs during cyclical transmission of *Trypanosoma brucei*. PLOS Pathogens **1**: 225—231

Van den Abbeele J, Claes Y, Van Bockstaele D, Le Ray D, Coosemans M (1999) *Trypanosoma brucei* spp development in the tsetse fly: characterisation of the post-mesocyclic stages in the foregut and proboscis. Parasitology **118**: 469—478

Van Hellemond JJ, Opperdoes FR, Tielens AG (2005) The extraordinary mitochondrion and unusual citric acid cycle in *Trypanosoma brucei*. Biochem Soc Trans **33**: 967—971

Vassella E, Reuner B, Yutzy B, Boshart M (1997) Differentiation of African trypanosomes is controlled by a density sensing mechanism which signals cell cycle arrest via the cAMP pathway. J Cell Sci **110**: 2661—2671

Vickerman K (1985) Developmental cycles and biology of pathogenic trypanosomes. Br Med Bull **41**: 105—114

Vickerman K, Tetley L, Hendry K, Turner C (1988) Biology of African trypanosomes in the tsetse fly. Biol Cell **64**: 109—119

Woodward R, Gull K (1990) Timing of nuclear and kinetoplast DNA replication and early morphological events in the cell cycle of *Trypanosoma brucei*. J Cell Sci **95**: 49—57

Ziegelbauer K, Quinten M, Schwarz H, Pearson T, Overath P (1990) Synchronous differentiation of *Trypanosoma brucei* from bloodstream to procyclic forms *in vitro*. Eur J Biochem **192**: 373—378